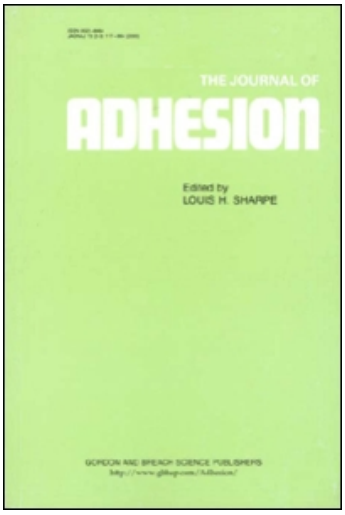

The Journal of Adhesion
Publication details, including instructions for authors and subscription information:
http://www.informaworld.com/smpp/title~content=t713453635

Fracture Toughness of a Silane Coupled Polymer-Metal Interface: Silane Concentration Effects

Douglas H. Berry[a]; Apinan Namkanisorn[b]
[a] Boeing Commercial Airplanes, The Boeing Company, Seattle, Washington, USA [b] Department of Chemical Engineering, Faculty of Engineering, King Mongkut's Institute of Technology, Ladkrabang Chalongkrung Road, Ladkrabang, Bangkok, Thailand

To cite this Article Berry, Douglas H. and Namkanisorn, Apinan(2005) 'Fracture Toughness of a Silane Coupled Polymer-Metal Interface: Silane Concentration Effects', The Journal of Adhesion, 81: 3, 347 — 370
To link to this Article: DOI: 10.1080/00218460590944657
URL: http://dx.doi.org/10.1080/00218460590944657

The Journal of Adhesion, 81:347–370, 2005

ISSN: 0021-8464 print/1545-5823 online
DOI: 10.1080/00218460590944657

Taylor & Francis
Taylor & Francis Group

Fracture Toughness of a Silane Coupled Polymer-Metal Interface: Silane Concentration Effects

Douglas H. Berry
Boeing Commercial Airplanes, The Boeing Company, Seattle, Washington, USA

Apinan Namkanisorn
Department of Chemical Engineering, Faculty of Engineering, King Mongkut's Institute of Technology, Ladkrabang Chalongkrung Road, Ladkrabang, Bangkok, Thailand

Fracture toughness of joints made from a glassy, 343,000 molecular weight polystyrene block bonded to chromic-sulfuric acid etched or phosphoric acid anodized aluminum are investigated. The fracture tests are performed with a 90-degree peel apparatus under "dry" laboratory conditions and "wet" conditions created by submerging the apparatus in a temperature controlled water bath. The bond strengths are controlled using various concentrations of styrl silane coupling agent added directly into the styrene monomer solution that polymerizes against the aluminum. Ellipsometric measurements on smooth silicon surfaces verify that the thickness of bound polymer is controlled by the silane to polystyrene mole ratio. X-ray photoelectron spectroscopy (XPS) analysis of fractured surfaces indicates that the fracture is near the aluminum surface. Both the wet and dry fracture energy as a function of bound polymer thickness on acid etched aluminum joints resemble quite closely the adhesion literature results obtained by fracturing pairs of fused, immiscible glassy polymers. Reasons for this similarity are discussed.

Keywords: Polymer-metal adhesion; Fracture mechanics; Silane coupling agent; Glassy polymers

Received 14 September 2004; in final form 12 January 2005.

This paper is one of a collection of articles honoring Manoj Chaudhury, the recipient in February 2005 of *The Adhesion Society Award for Excellence in Adhesion Science, Sponsored by 3M*.

Both authors would like to thank Prof. Manoj Chaudhury for the use of his laboratory in the Department of Chemical Engineering at Lehigh University to perform the experimental portion of this work, and then for his helpful comments and insight in the writing of this article. Financial support for this work, provided by The Boeing Company and the Polymer Interface Center at Lehigh University, is gratefully acknowledged.

Address correspondence to Douglas H. Berry, The Boeing Company, P.O. Box 3707, M/C OM-FM, Seattle, WA 98124-2207, USA. E-mail: douglas.h.berry@boeing.com

INTRODUCTION

Polymer-metal adhesive joints are currently used in numerous applications, including many associated with the aerospace and automotive industries. More widespread use is expected in the future as advanced polymer-metal composites are introduced with a goal of increasing strength and fracture toughness, while reducing weight and eliminating galvanic corrosion potential between dissimilar materials. In general, the joining of polymeric materials, including composites, in bonded assemblies is becoming more widespread and important as aerospace manufacturers look for faster assembly methods, more durable and corrosion resistant products, and weight reduction.

For glassy polymer, plastic, or metal surface substrates most bonding to another material consists of a substrate surface pretreatment that usually chemically and mechanically prepares the surface for better receptivity followed by the addition of macromolecular "connector molecules" that can attach to the surface through either or both penetration and chemical reaction. These "connector molecules" can then react with any adjacent polymer through the mechanisms of (1) interpenetration into the adjacent phase and (2) chemical reaction and crosslinking with the adjacent material [1].

Bonding systems typically contain a crosslinked thermoset which is glassy at normal operating temperatures. The most typical for aerospace applications, especially structural, is modified epoxy based resin. Occasionally thermoplastic polymers, such as polyether-ketone-ketone (PEKK), polyphenylene-sulphide (PPS), and polyimide derivatives are used as reinforced thermoplastic laminates in semi-structural aerospace applications involving composite to metal bonding. These thermoplastics generally have 25–50% crystallinity to prevent creep and have the advantage of lower temperatures and less severe processing conditions such as no vacuum bag, resulting in considerable process and material savings [2].

Independent of the exact system, a major problem with specification and use of joints containing adhesive bonding in performance structures is durability following exposure to moisture or high humidity at elevated temperatures. In polymer-metal joints, various modes of degradation may occur under environmental exposure such as deterioration of the polymer or metal near the interface [3] and modification of the interfacial zone [4]. Frequently, the locus of failure of well prepared polymer-metal joints change from cohesive mode in the adhesive layer to an apparent interfacial mode following environmental exposure, and the change in failure locus is accompanied with a reduction in joint strength [5]. The exact transition point from

adhesive to cohesive failure appears to be crack velocity, humidity, surface pretreatment, and polymer related [6].

Both surface topology and surface chemistry play vital roles in polymer-metal joint performance. Rider and Arnott used an ultra milling technique to show that change in metal micro-roughness can lead to a two decade change in the fracture toughness of aluminum-epoxy joints [7]. Zhang et al. [8], using a different epoxy system, started with one μm diamond polished aluminum and created micro-roughness using both SiC grinding paper ranging from 60 to 600 grit and an oxidation process. They found that the twenty fold increase in fracture energy correlated in non-linear fashion with a roughness index measured by a profilometer with 0.25 micron scale resolution, rather than an atomic force microscope (AFM) with nanometer size resolution. Zhang et al. further concluded that fracture enhancement is not just due to an increase in contact surface area between epoxy and aluminum, but also the change of local mode-mixity as well as bridging and friction behind the crack. Both these studies were done under "dry" laboratory conditions.

The type of oxide on the metal surface is certainly important in wet conditions as the oxide can prevent or limit metal hydrolysis and also contribute to surface topology [3]. Surface oxide preparation techniques for aluminum range from simple detergent cleaning to the more chemically complex treatments of acid etching and anodizing. Bonding between polymer and metal can be greatly enhanced through coupling agents, such as silanes [9] and sol-gels [10], which are designed to react with both the organic polymer and inorganic metal surface as well as forming a hydrophobic interface.

Not only does the fracture of a polymer-metal joint involve interfacial chemical bonding and physical interactions on the order of one nanometer, but also mechanical deformation of polymer entanglements on the order of ten nanometers, and elastic/plastic deformation such as in crazing of the order of one hundred nanometers. Consequently, how the interfacial fracture processes are coupled to the bulk energy dissipative processes is of considerable importance for a fundamental understanding of the molecular and micro-mechanical processes that impart strength and stability to the adhesive joint when stressed under various environmental conditions of moisture and temperature. This understanding is also important in identifying suitable accelerated aging tests [6]. Many findings from a study of bonding between a polymer-metal joint are also applicable to interface and interphase adhesion enhancement in adhesive bonding between polymers, particularly those related to interfacial chemical bonding and energy dissipative processes in the adhesive [1].

In this paper, the interfacial bonding conditions needed for adequate polymer-metal joint fracture resistance and micro-mechanisms involved in fracture of the polymer-metal joint under dry and wet environmental conditions are examined. A model system of a thick block of high molecular weight polystyrene is chemically bonded to a thin film of high purity aluminum pretreated with chromic-sulfuric acid etched or phosphoric acid anodized surface preparations. Since the polystyrene only weakly bonds with oxide layers on aluminum through non-specific Van der Waals interactions, the extent of specific chemical bonding is controlled using small amounts of a styrl silane coupling agent. The strength of the joint is then tested in a 90-degree peel test under "dry" laboratory conditions and "wet" conditions created by submerging the test in a temperature controlled water bath. By varying the load used to peel the aluminum from the polystyrene block, the crack growth rate can be controlled from gradual sub critical crack growth to rapid failure. The mole ratio of silane to polystyrene is varied from zero to about one and the fracture energy at higher crack velocities of around 0.1 mm/s are studied in order to determine the minimum mole ratio as well as thickness of chemically bound polystyrene needed to provide toughness for a joint. Fracture energy results are compared to those obtained for the toughness of interfaces obtained from fused, immiscible, glassy polymers [11, 12] and discussed in terms of concepts developed to explain the toughness of these joints including chain pullout, chain scission, and partially complete craze formation [13–15].

EXPERIMENTAL

Experimental materials and conditions are described in further detail in reference [16].

Materials

Aluminum foil (Al 1145 NP; composition in weight %: 99.45 Al min., 0.55 max. of Si and Fe combined, 0.05 max. of Cu, Mg, Mn, V, and Zn) was cut into 38 mm wide by 76 mm long by 0.075 mm strips prior to surface pretreatment. Polystyrene (PS) was synthesized using styrene monomer (99% pure), and 2,2′-Azobisisobutyronitrile (AIBN) initiator from Aldrich Chemical Company. The styrl functional silane coupling agent used to vary the interfacial strength of the joints was Dow Corning Z-6032®, $CH_2{=}CHC_6H_4CH_2NH(CH_2)_2NH(CH_2)_3Si(OCH_3)_3{\cdot}HCl$ with a molecular weight M_w of 375 [17].

Surface Pretreatments and Joint Preparation

Surface pretreatment methods used were those typical for chromic-sulfuric acid etching [18] and phosphoric acid anodization [3, 19]. All strips were thoroughly rinsed with deionized and distilled water and dried in air after the preparations. For the acid etched preparation, the aluminum strips were immersed for 12 minutes in an aqueous solution held at 58°C containing sodium dichromate, sulfuric acid, and water in a 1:10:30 ratio by weight. In the anodize preparation, aluminum strips were clamped into a specimen holder and immersed in a 10 wt% phosphoric acid electrolyte at room temperature. A constant anodizing current of 100 mA was then applied to the samples for 30 minutes.

24 g styrene monomer purified of inhibitor, 0.1 g AIBN initiator, and the appropriate amount of Dow Corning® Z-6032 silane, which was varied between 0 and 20 microliters, were mixed in a beaker and stirred thoroughly for 30 minutes. A rectangular, Teflon mold was clamped to the aluminum foil and filled with the mixture. The assembly was then placed in a Petri dish, held at 75°C for 8 hours under a nitrogen atmosphere, and then cooled in the oven overnight. The mold was removed and a joint consisting of a 2.5 mm block of PS bonded to a 0.075 mm film of aluminum was produced. The resulting polystyrene had an average molecular weight M_w of 343,000 as determined by gel permeation chromatography. Using a film made from a solution containing 5 microliters of styrl silane equivalent to a silane to polystyrene mole ratio of 0.17, a glass transition temperature T_g of 99°C was determined using a Rheometrics RDA II dynamic mechanical analyzer (TA Instruments, New Castle, DE, USA).

Normally a silane is made up in a dilute solution, applied as a thin coat onto the surface by dipping the aluminum or painting the silane, and then cured at elevated temperature onto the surface [20]. However in this study the silane was added into the mixture because this method produced better reproducibility in the strength of the joints and allowed for better control over the distribution of the silane into the polystyrene. Also using this procedure produced joints that gave no significant difference in terms of crack propagation velocity at a given applied load between freshly prepared samples and samples that were stored in ambient laboratory conditions for up to 7 days, indicating that the silane ester was completely hydrolyzed when it reacted with the aluminum surface.

Joint Surface Analysis

XPS analysis of PS and aluminum surfaces was performed on a SCIENTA ESCA-300 instrument (Gammadata Scienta AB, Uppsula,

Sweden). The exciting radiation of this instrument was provided by a monochromatic Al K_α X-ray source ($h\nu = 1486.6$ eV) operated at a constant power of 4.5 kW and pass energy of 300 eV. All spectra were taken at a 90-degree take-off angle. An electron flood gun was used to neutralize the surface charge of the specimen. Data analysis was performed for O_{1s}, Al_{2p}, C_{1s}, P_{2s}, and Si_{2p} peaks using SCIENTA's analysis software where the binding energy of each atom was referenced to the binding energy of C_{1s} (285 eV).

A JEOL-6300 SEM microscope (JEOL Ltd, Tokyo, Japan), operating at accelerating voltages of 3–10 kV, was utilized to examine the topography of the oxide layer on aluminum foils. A gold coating, approximately 15 nanometers thick, was sputtered onto all samples from the PS side of the fractured joint to eliminate any electron charging effects. A similar procedure was performed on the aluminum side when a thick layer of PS was present, such as in the dry peel condition. Transmission electron microscopy was performed on a Philips-420 TEM microscope (FEI, Hillsboro, OR, USA), operating at the accelerating voltage of 100 kV. Samples for TEM were prepared using the procedure of Shimizu, et al. [21].

Joint Interphase Morphology

TEMs of the two types of joints are shown in Figure 1. These specimens were prepared using an ultramicrotomy technique [21] requiring

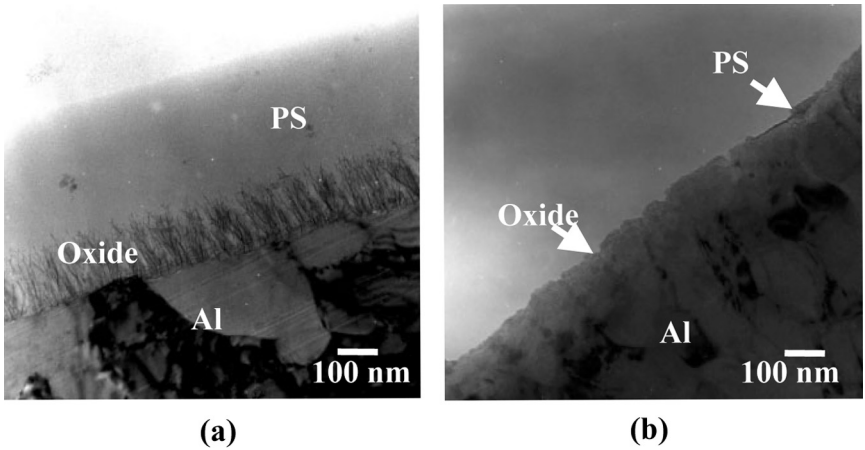

FIGURE 1 TEM images showing the interphase region between PS-Al joints after ultramicrotomy for (a) phosphoric acid anodized and (b) chromic sulfuric acid etched surface pretreatments.

40 nm thin sections cut with a diamond knife so the polystyrene thickness in the sample preparation was reduced to 0.5 mm. The acid anodized joint in Figure 1a shows that much of the PS layer remains intact with the branched oxide layer. No voids are evident suggesting intensive mechanical interlocking of the polymer with the oxide surface. The thickness of the oxide layer increases by about 20% as it branches into the polystyrene and appears as loose branches compared to the anodized oxide layer without PS [16]. The acid etched joint in Figure 1b shows a much thinner oxide layer and much of the PS layer is removed by the diamond knife.

If the oxide has a characteristic pore diameter smaller or not much larger than the size of the polymer then total penetration of the polymer into the oxide pores is not always possible due to the existence of back pressure stemming from air entrapped in these pores [22]. To determine if this was the case for the acid etched, joints, the aluminum was etched away by immersion of the joint in sodium hydroxide solution for 5 minutes. This left a very thin layer of black oxide that could be removed in an ultrasonic bath containing distilled water, while leaving the PS surface that had been facing the aluminum essentially unaffected. SEMs of the aluminum surface after acid etch treatment (Figure 2a) and then of the PS surface facing the aluminum after joint formation and then etching away of the aluminum by NaOH (Figure 2b) show that the PS does penetrate into the pores of the aluminum. The morphology of PS contains hillocks that are replica of the porous aluminum oxide layer. The length scale of the hillocks is roughly the same as that of the porous oxide layer and suggests the potential for mild mechanical interlocking.

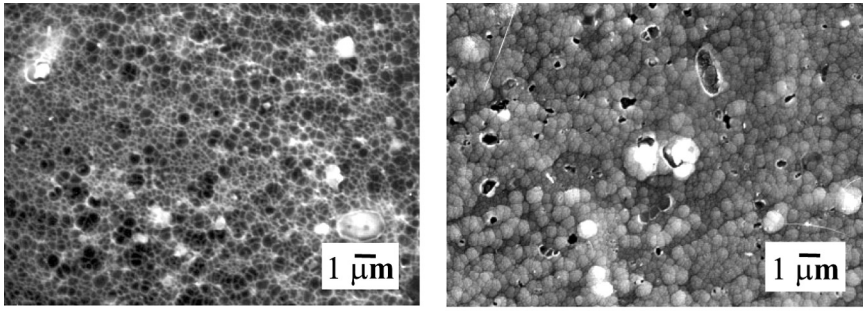

FIGURE 2 SEM images showing evidence of PS penetration into Al oxide structures. (a) Al surface after acid etched pretreatment and (b) PS surface after Al etched away using NaOH.

Fracture Mechanics Test

A 90-degree peel test was carried out using the apparatus illustrated in Figure 3. After peeling part of the aluminum foil from the polystyrene, a dead load was hung from the free end of the foil. The entire assembly was placed into the PYREX® kettle containing water or air maintained at the test temperature. After an induction period lasting from 2–24 hours, the crack propagated at a constant rate determined by the applied load. The crack front was monitored by the video-microscope set up as shown in Figure 3. The fracture energy (G) was calculated from the peel force per unit width (P) using

$$G = P \cdot (1 - \cos\theta) \tag{1}$$

where θ is the peel angle, 90°. The force acting on the aluminum film was corrected for the buoyancy force and for plastic deformation of the

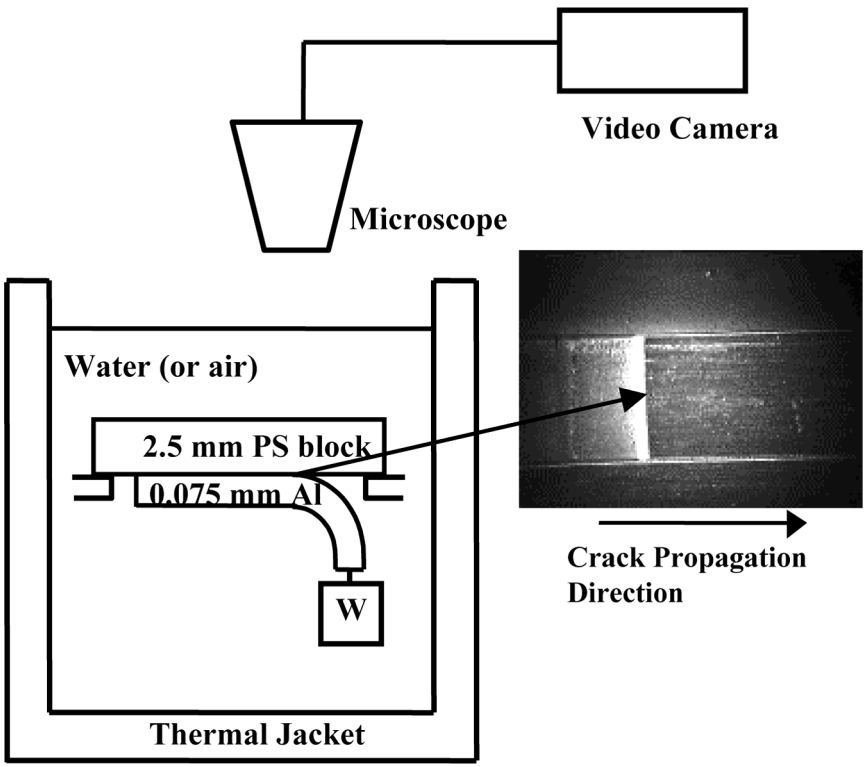

FIGURE 3 Schematic of hygrothermal peel test apparatus with optical micrograph showing crack front.

aluminum [16]. By peeling away the thin aluminum from the thicker polystyrene block the crack tended to propagate along the joint interface.

RESULTS AND DISCUSSION

Role of Silane Coupling Agent in Bonding Polystyrene to Aluminum

The styrl functional silane coupling agent was varied from zero to 2.1×10^{-2} mol% based on the molecular weight of styrene monomer or zero to 0.69 when expressed as the mole ratio (MR) of silane to polystyrene. There is strong evidence that the styrl silane reacted with both the aluminum and polystyrene and provided anchoring points based on dry fracture, solvent extraction, and PS fusion tests at low and high MR [16]. The silane is expected to incorporate into PS through the active styrl double bond via the normal free radical polymerization process. Some of the silane should also adsorb on and react with the aluminum surface via one of the three alkoxy group on its opposite end [23] as in Figure 4 and the following equation:

$$\mathrm{R{-}Si(OCH_3) + HOAl \rightarrow R{-}Si{-}O{-}Al + CH_3OH} \qquad (2)$$

After condensing with the aluminum surface, the remaining silanol groups are capable of hydrogen bonding or condensing with adjacent silanol groups from another silane if they are nearby. The silane provides the grafting molecule between the aluminum surface and the PS chains growing in the bulk via a free radical mechanism. Entanglement of these surface grafted PS chains with the bulk PS matrix chains also growing via free radical addition gives the joint adhesive strength. Entanglements in the bulk PS give the joint cohesive strength.

Role of Silane in Determining Thickness of Grafted Polystyrene Layer

An accurate thickness of a polystyrene layer grafted to aluminum was difficult to determine because of the roughness of the substrate. As a substitute, 1-mm thick blocks of polystyrene were bonded to polished silicon wafers using various mole ratios via the same free radical polymerization process. After overnight Soxhlet extraction with toluene, the remaining bound polystyrene could be measured using ellipsometry [16]. The results are shown in Figure 5 where the measured grafted layer thickness (t_p) is plotted versus the square root of the silane to polystyrene mole ratio. The best fit line yields the equation

$$t_p = 14.24 * (MR)^{1/2} + 3.02 \qquad (3)$$

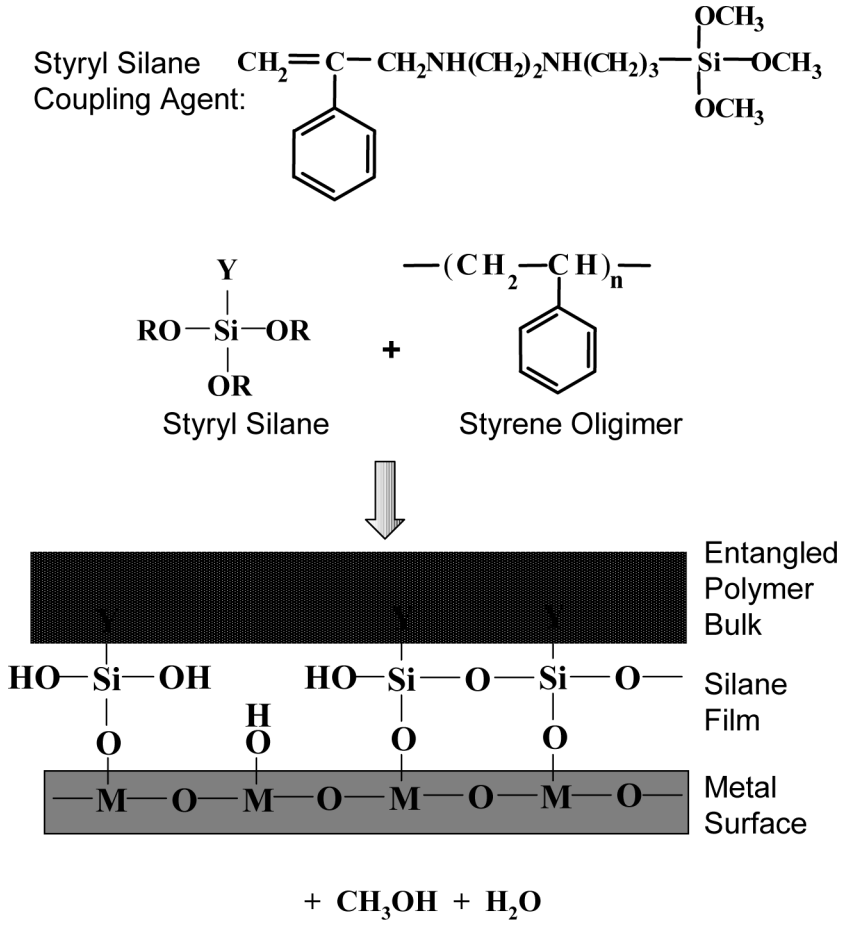

FIGURE 4 Schematic of silane coupling reaction between polystyrene and aluminum.

and produces a correlation coefficient of 0.97. The square root dependence on MR might be expected if the silane is acting as a coupling agent since the polystyrene is covering a planar wafer surface. Even without any silane, a small amount of polystyrene was physisorbed onto the silicon wafer giving a measured thickness of 2.7 nm and an estimated thickness based on Equation (3) of 3.0 nm. At mole ratios above about 4.5, the polystyrene forms a gel structure that swelled during solvent extraction so t_p could no longer be measured.

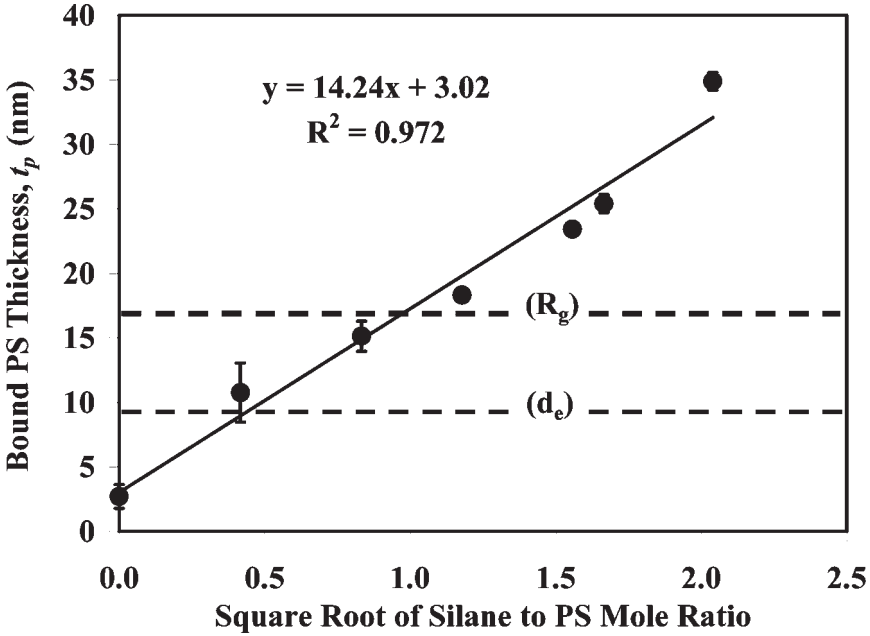

FIGURE 5 Ellipsometric measurement of polystyrene thickness (t_p) bonded to a polished silicon wafer after toluene extraction versus square root of silane to polystyrene mole ratio (MR). Straight line is best statistical fit via a linear regression analysis.

The radius of gyration R_g of bulk polystyrene (PS) can be estimated as 16.5 nm using the relation

$$R_g^2 = \frac{C_\infty M_w l_o^2}{6 m_o} \tag{4}$$

where M_w is the average PS molecular weight, l_o is the length of a C–C bond (0.154 nm), m_o is the molar mass per backbone bond (52 for PS), and C_∞ is 10.5 at 20 to 25°C [24]. The predicted mole ratio producing t_p equal to R_g is 0.90 from the correlation line of Equation (3) and Figure 5.

The average distance between entanglements in bulk PS is estimated as 9.3 nm from

$$d_e^2 = \frac{C_\infty M_e l_o^2}{m_o} \tag{5}$$

where M_e is the average molecular weight between entanglements (18,000 for PS [25]). The predicted mole ratio producing t_p equal to d_e is 0.20 from the correlation line of Equation 3.

Locus of Failure Analysis

XPS data indicates that the source for improved wet strength achieved with styrl silane addition is due to near surface interaction of the polystyrene with the aluminum substrate. Figure 6a shows changes in the aluminum Al_{2p} peak at 73 eV and Figure 6b shows changes in the carbon C_{1s} at 285 eV on the acid etched aluminum side of fractured surfaces of a joint made with a mole ratio of 0.17 and peeled at 22°C in water. From Figure 6a, the size of the Al_{2p} peak is largest at the lowest fracture energy of 173 J/m^2 with a crack propagation velocity less than 0.002 mm/sec and is smallest at the highest wet fracture energy of 1268 J/m^2 with a crack propagation velocity greater than 0.1 mm/sec. Under dry conditions, the peak is almost non-existent. Similar results although not as pronounced were also obtained by performing a detailed scan at 99.2 eV, characteristic of metallic Si inclusions [26].

The C_{1s} peak in Figure 6b has the opposite behavior with the peak largest at the highest wet fracture energy or under dry conditions and the smallest at the lowest fracture energy condition. In addition, the carbon shake-up peak at 291.7 eV, representing a π-π^* molecular orbital transition becomes apparent at the higher fracture energies. This peak is usually used to identify aromatic or unsaturated moieties in the polymer backbone or side chains and can be observed in a control spectrum acquired from polystyrene so the presence of the shake-up peak indicates that the polystyrene coverage on the high fracture energy aluminum surfaces becomes quite thick. Taken together the detailed Al_{2p} and C_{1s} scans show that the fracture is nearly interfacial at low fracture energies, but still has a small component of polystyrene, and is close to cohesive at high fracture energies. XPS analysis of the PS side of the fractured joint showed no remnants of aluminum, confirming that the cohesive fracture does not occur within the oxide layer present on aluminum [16].

Distribution of Silane on Polystyrene

The change in PS grafted thickness with MR in Figure 5 and the change in the locus of failure in Figures 6a and 6b does not conclusively demonstrate how the silane coupling agent is distributed on the PS molecules. The data in Figures 6a and 6b suggests that the silane on a PS molecule near the aluminum surface will react almost irreversibly with the aluminum oxide and stay anchored. The data in Figure 5 suggest that the silane is incorporated randomly into the forming styrene molecules during the reaction. Product literature data indicates that the styrl silane should have similar reactivity as styrene

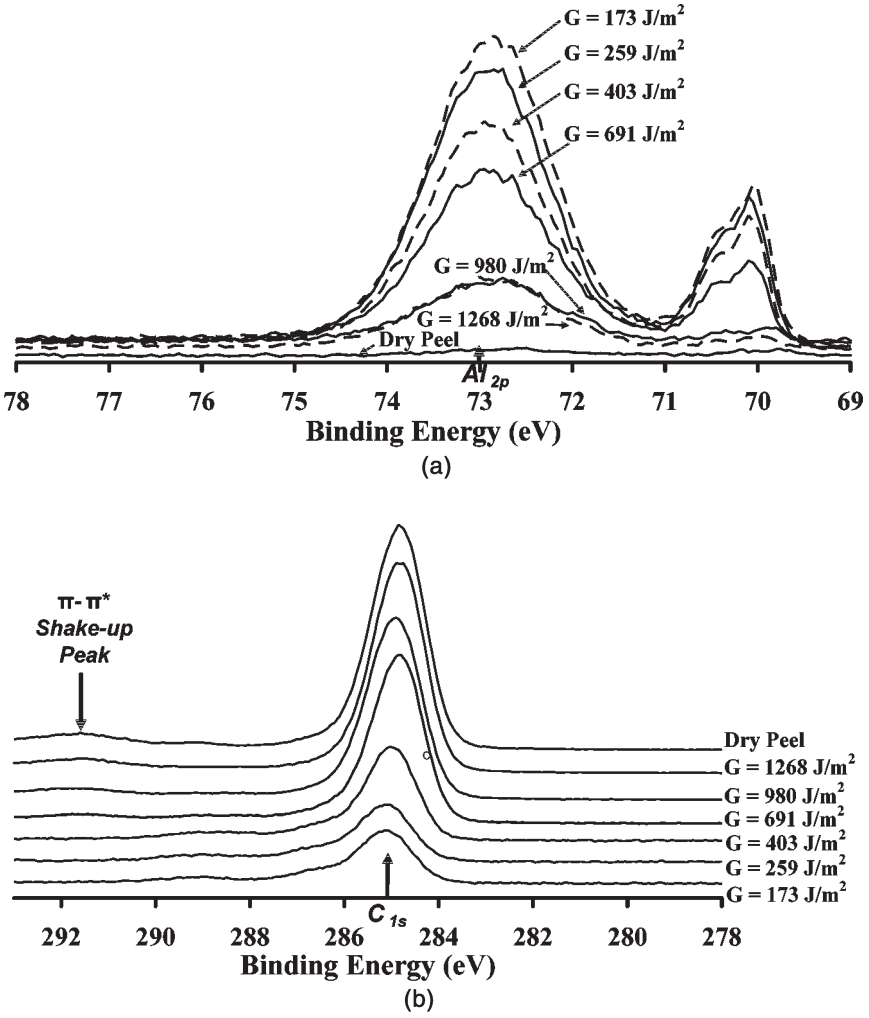

FIGURE 6 (a) XPS data of Al_{2p} peak at 73 eV as a function of fracture energy (G) for a joint at 0.17MR on acid etched aluminum. Joints peeled in water at 22°C. (b) XPS data of C_{1s} peak at 285 eV as a function of fracture energy (G) for a joint at 0.17MR on acid etched aluminum. At high fracture energies the shake-up peak at 291.7 eV indicative of bulk polystyrene structure appears. Joints peeled in water at 22°C.

monomer [17]. If many silane molecules were to attach to a single PS molecule and then react with the oxide surface the movement of the PS molecule would be severely hindered and the thickness of the

bound PS layer at MR equal to one would be expected to be much less than R_g. At MR equal to one there is one silane coupling agent molecule to every 3360 styrene monomers so if the silane does randomly incorporate into the PS molecule then the distribution of silane to PS molecules should form a Poisson curve [27]

$$\Pr(y) = \frac{e^{-\eta}\eta^{y}}{y!} \tag{6}$$

Here, $\Pr(y)$is the probability of having y silane molecules on a PS molecule and η is the MR for the solution. The distribution for various values of MR between 0.01 and 1.0 is shown in Figure 7. The probability of having more than one coupling agent on a single PS molecule is less than 5% until MR is greater than 0.35. At MR equal to 0.7, the probability of a PS molecule having two silane molecules becomes greater then 10% but the probability of three stays less than 3%. At MR equal to one, the probability of three silanes on a single molecule

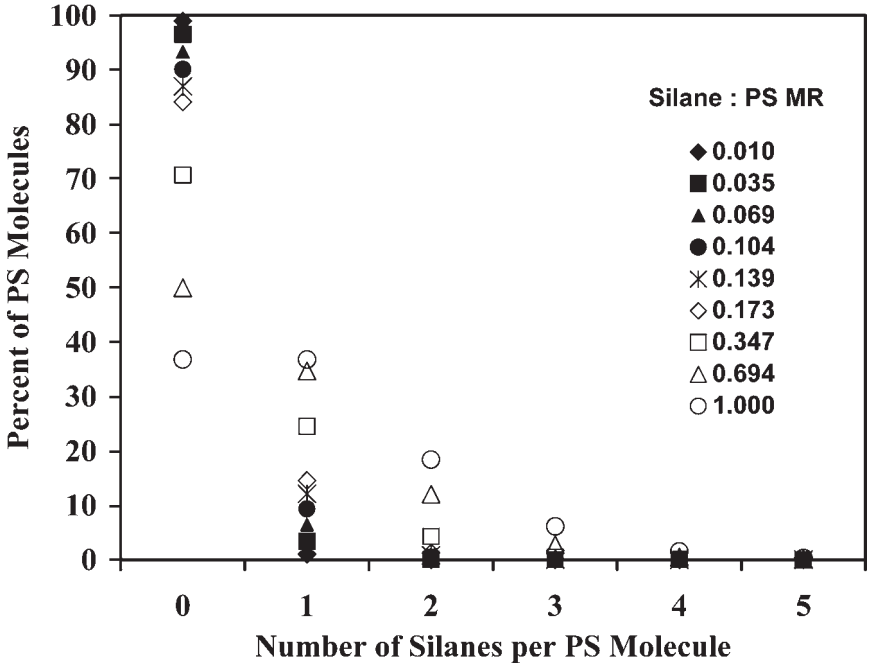

FIGURE 7 Probability distributions of silanes on a PS molecule as a function of silane to polystyrene mole ratio (MR) assuming a poisson distribution. Mole ratios between 0.035 and 0.694 correspond to experimental values tested in fracture experiments.

is slightly greater than 6%. Thus the model suggested here is that of PS molecules bound by single silane molecules to the aluminum surface. Only at higher MR, above 0.35 MR, is there much chance of multiple silanes on a single molecule, or much chance of silanol groups from different silanes condensed on the aluminum surface forming cooperative attachments through hydrogen bonding or condensation with each other.

Previously, a cooperative bonding model between condensed silanes on the same or different polystyrene molecules was suggested [16] and might still be valid. This could conceivably happen if the condensation reaction of equation (2) is much more rapid than the free radical reaction incorporating the styrl silane into the polystyrene. However, the square root dependence of grafted polystyrene thickness versus mole ratio in Figure 5 would not seem to support this hypothesis.

Effect of Silane Coupling Agent Concentration at Higher Peel Velocity

Previously, the joint fracture energy was investigated in room temperature air (dry) and water (wet) at silane concentrations above 0.0053 mol% (based on styrene monomer) or PS to silane mole ratios above 0.17 [16]. Under dry conditions, the limiting cohesive fracture energy of approximately $1700\,J/m^2$ was almost independent of peel velocity and aluminum surface pretreatment. Under wet conditions, the fracture energy became velocity and pretreatment dependent, but reached the plateau cohesive fracture energy of a little over $1300\,J/m^2$ in all cases at peel velocities above 0.1 mm/s. The difference between wet and dry peel strength at high velocity is probably because water plasticizes the PS. From Figure 5, the lowest mole ratio used was only slightly less than the 0.20 MR necessary to produce a grafted PS layer thickness t_p equivalent to d_e.

Additional experiments were performed at lower silane concentrations under dry and wet conditions on joints with an aluminum acid etched surface. Results for the wet conditions are shown in Figure 8 and cover MR from 0.035 to 0.69, a factor of 20. For MR less than 0.17 the high velocity plateau for fracture energy is approached at a slower rate as a function of velocity, but the interpolated value at 0.1 mm/s was still used as there was data available for all mole ratios.

This high velocity fracture energy as a function of silane to polystyrene MR is shown in Figure 9 for the acid etched pretreatment when tested under both dry and wet conditions. At zero MR the joint exhibited very minimal adhesion with fracture energy of less than $1\ J/m^2$ when tested in water at 22°C, while at 0.035 MR the tested

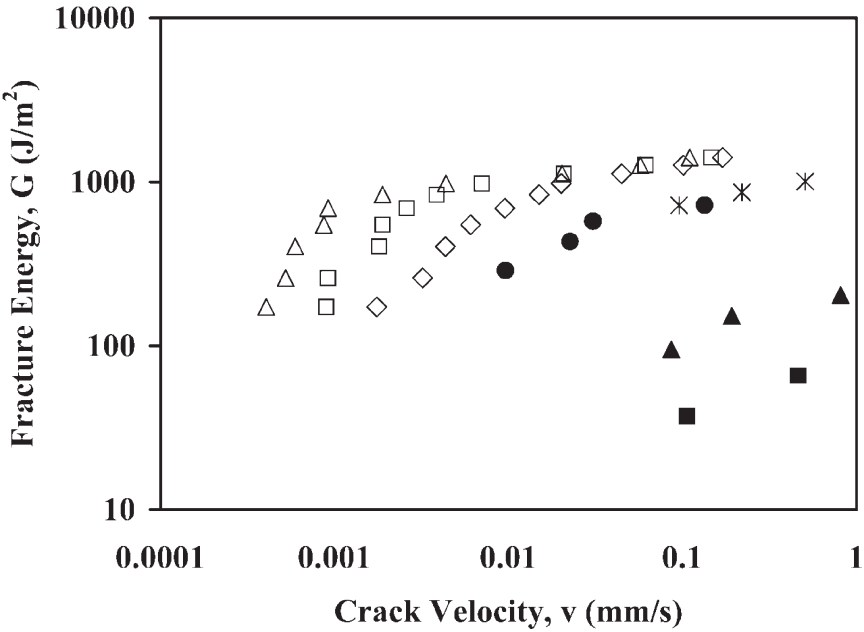

FIGURE 8 Fracture energy of acid etched Al joints made with MR from 0.035–0.069 as a function of crack propagation velocity. Peel tests were performed in water at 22°C. MR plotted: ■, 0.035; ▲, 0.069; ●, 0.104; ∗ , 0.139; ◇, 0.173; □, 0.347; △, 0.694.

joint had fracture energy of $37\,J/m^2$. The dry joint tested in air having no silane coupling agent did have a small fracture energy of $32\,J/m^2$, but this was still a factor of 50 lower than the joints made with MR greater than 0.17. Also shown in Figure 9 are fracture values for joints made with acid anodized pretreatment of the aluminum and then tested dry in air. Even with no silane coupling agent, the fracture energy of the anodized joint $1340\,J/m^2$ was close to the maximum value of the joints made with acid etched pretreatment on the aluminum and tested under wet conditions. An anodized joint made at 0.17 MR had dry fracture energy of $1760\,J/m^2$ just slightly in excess of the acid etched joints made above 0.17 MR and tested dry. Results for an anodized joint under wet conditions cannot be shown because the aluminum corroded before the joint failed.

Fracture Regimes at High Peel Velocity

Schnell, Stamm, and Creton [11, 12] have studied high velocity fracture toughness between high molecular weight styrene-based

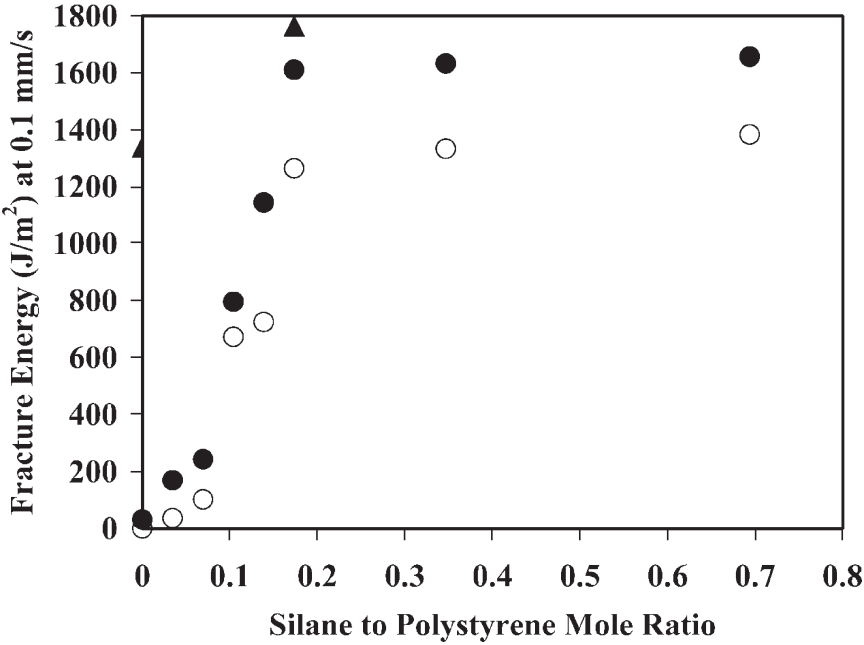

FIGURE 9 Fracture energy at high crack propagation velocity versus MR using acid etched and acid anodized aluminum tested under 22°C dry and wet conditions (○, etched wet; ●, etched dry; ▲, anodized dry).

homopolymer blocks using asymmetric double cantilever beams. They found that as the width of the interface between the homopolymers measured by neutron reflectivity increased from 6 to 12 nm, the fracture toughness increased by a factor of 30. Three regimes were identified. Regime I below 6 nm width showed practically no change in fracture toughness. They ascribed the fracture mechanism here as due to chain pullout (disentanglement). In Regime II, between 6 and 12 nm interfacial widths, the fracture toughness increased dramatically. A plastic zone was formed ahead of the crack tip during crack propagation and the increase in toughness was attributed to increasing entanglements between the homopolymer blocks with chain scission occurring in the plastic zone. Finally in Regime III, above 12 nm width, craze formation is prevalent. The fracture toughness became independent of interfacial width and equal to the bulk material value. Because regime II was centered about d_e, they concluded that d_e (not R_g) was the minimum interpenetration needed at the interface to sustain a stress identical with the stress that could be sustained by any arbitrary plane in the polymer bulk.

More recently, Silvestri and coworkers [15] proposed a more complete mathematical model in which there are still three regimes, but with somewhat different interfacial width ranges. At small widths, the dominant failure mechanism is chain scission. In the intermediate regime, the fracture mechanism is due to partial crazing, where at least some of the load bearing strands in the forming craze fail by chain scission during plastic deformation in the crack tip so the craze cannot fully develop. Excellent agreement was obtained with data from Brown [28] for the toughness of an interface between polymethylmethacrylate (PMMA) and a random copolymer based on PS and PMMA. Agreement with the styrene based homopolymer data [11] was less satisfactory with a prediction of a much smaller value than 9 nm for the critical width. Silvestri [15] suggests that the discrepancy might be because the entanglement density in the presence of an interface should be sharply reduced leading to a smaller interfacial width than is necessary for full craze development.

If the data in Figure 9 is re-plotted using the best fit line (equation 3), the three regimes shown in Figure 10 for the acid etched aluminum joint results are similar to those identified by Schnell et al. [11, 12]. Here the transitions between regimes arise from the interactions or inter-diffusion of the polystyrene grafted layer thickness t_p on the aluminum with the bulk polystyrene. At sufficiently small t_p, entanglement between the bulk polymer and grafted layer attached to the aluminum by styrl silane coupling agent cannot occur (Regime I). While the fracture energy is always greater for the dry acid etched aluminum than for the wet at a given t_p, the two conditions give similar shaped curves. The transition points between regimes depend slightly on the test condition but are about 5 nm for Regime I to II and about 9.5 nm for Regime II to III. These transition points are only slightly different than those found for fracture toughness between the styrene based homopolymers [12].

Optical micrographs of the polystyrene side of the peeled joints are shown in Figure 11. At low silane coverage (Regime I), no polymer roughness (or crazing) is apparent. Polymer chain pull out only in either dry or wet condition probably occurs although Silvestri et al. [15] would attribute the fracture energy to chain scission. The chain scission here could occur between carbon atoms in the polymer backbone or at the aluminum surface in the Al–O–Si bond. An additional mechanism, hydrolysis of the siloxane bond, is available in the wet condition which is not available in the dry condition or in the testing of the heat fused styrene homopolymer blocks of Stamm and coworkers [12]. For intermediate coverage (Regime II), more extensive, but intermittent polymer roughness appears. Fracture energy is

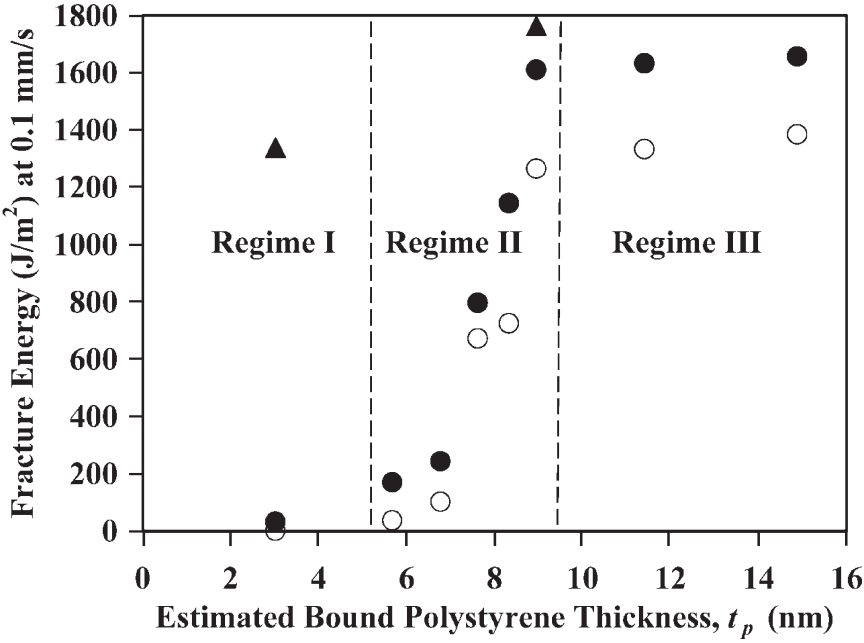

FIGURE 10 Fracture energy at high crack propagation velocity as a function of grafted polystyrene thickness using acid etched and acid anodized aluminum tested under 22°C dry and wet conditions (○, etched wet; ●, etched dry; ▲, anodized dry).

supplied by a combination of chain scission of the C−C bond in the main polystyrene chain, some chain pullout, and siloxane bond hydrolysis (wet only). Silvestri would attribute the primary fracture mechanism in this regime to partial craze formation. The start of ridge formation, which has a somewhat parabolic shape in the Regime II optical micrographs of Figure 11, might support the partial craze hypothesis. The ridges for the dry condition are more distinct than for the wet condition. At high coverage (Regime III), extensive roughness due to craze formation is evident, and the fracture energy is supplied solely by this mechanism. The optical micrographs for both wet and dry conditions show more defined ridges produced by the crazing and a sharper parabolic shape in this regime.

Wet to Dry Fracture Energy Ratio

Figure 12 shows the ratio of the wet to dry fracture energy as a function of predicted grafted polystyrene thickness. The ratio starts at

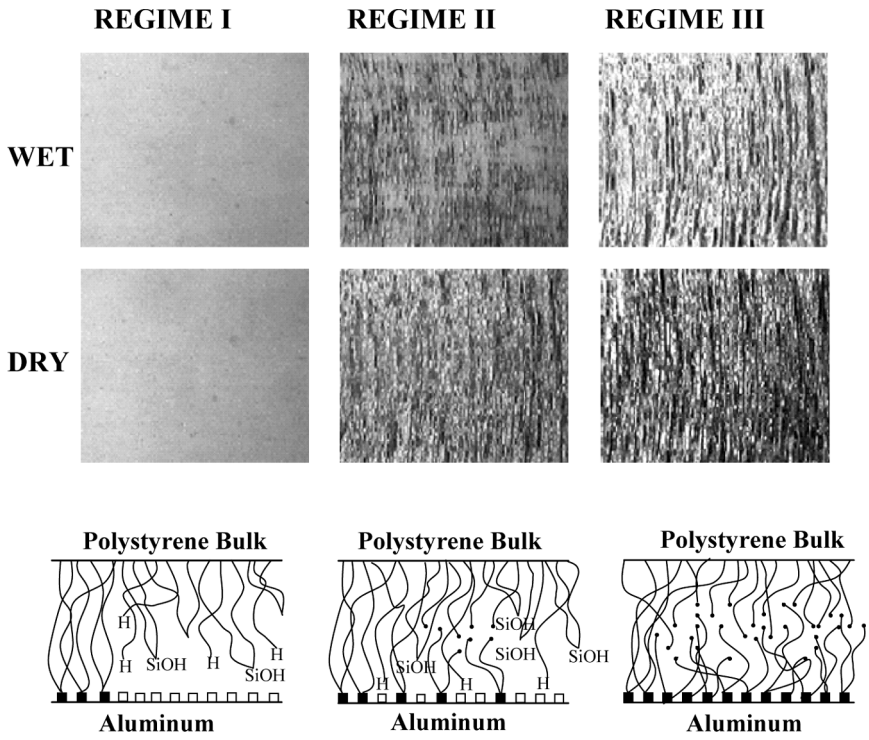

FIGURE 11 Optical micrographs of fractured, polystyrene surfaces on acid etched aluminum showing behavior in the three regimes of Figure 10. A schematic of the proposed fracture mechanism in each regime is shown. Regime I: chain pullout/hydrolysis; regime II: hydrolysis/pullout/scission; Regime III: chain scission from crazing.

close to zero in Regime I when no silane is present and seems to plateau at around 0.82 in Regime III. The relationship between this ratio and t_p appears almost linear in regime II although there is some scatter in the data. The other option is that the plateau is reached in what is currently designated as regime II and might then indicate that the partial crazing suggested by Silvestri [15] is indeed occurring and that the transition distance between regime II and III is less than d_e, perhaps because of the presence of the solid aluminum interface.

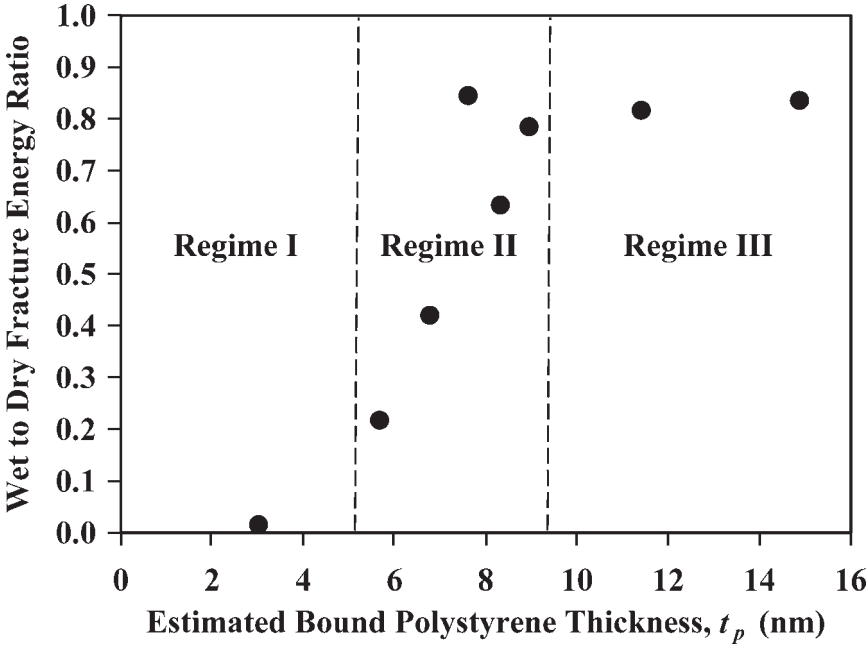

FIGURE 12 Wet to dry ratio of fracture energy as a function of grafted polystyrene thickness for acid etched aluminum joints tested at 22°C.

Effect of Surface Treatment on Fracture Regimes

The difference between the acid etched results in Figure 11 and the length scales given for the various regimes by Schnell et al. [11, 12] may be related to surface topography and moisture resistance of the aluminum surface. The high velocity limit fracture energy of joints made with anodized aluminum and containing either 0.0 or 0.17 mole ratio silane to polystyrene under dry condition is also indicated on Figures 9 and 10. There is only about 25% difference in the fracture energy between the two mole ratios. Figure 13 shows that there is also a larger dependence of fracture energy on crack propagation velocity for the acid etched than for the anodized aluminum joints under dry condition and a given mole ratio, either 0.0 or 0.17. There is pronounced fracture energy versus velocity dependence with an acid etched aluminum joint at 0.17 mole ratio tested under wet conditions. Results for an anodized joint under wet conditions cannot be shown because the aluminum corroded before the joint failed.

Typical SEMs and TEMs of the acid etched and anodized aluminum are found in reference [16]. The topography of the oxide layer in

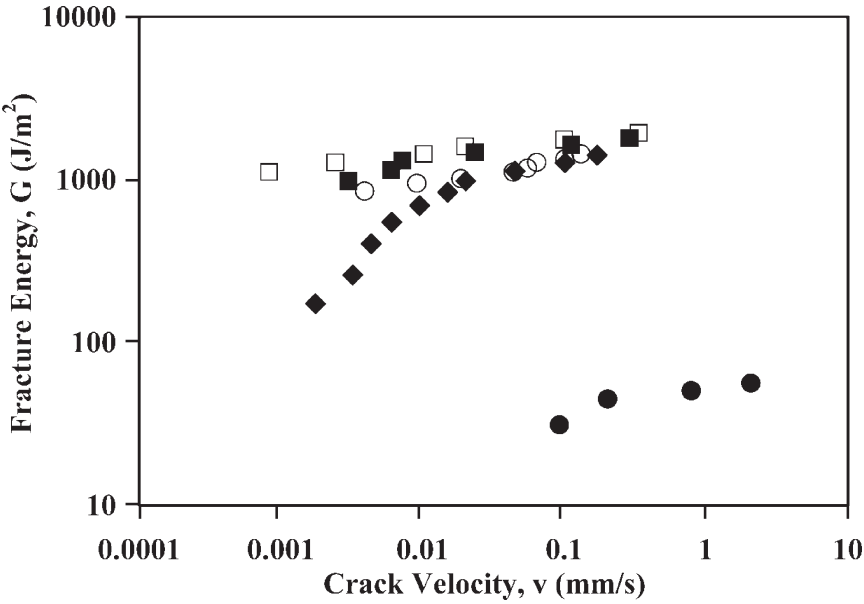

FIGURE 13 Comparison of fracture energy versus peel crack velocity for acid etched and anodized aluminum surfaces at 0.0 and 0.17 mole ratio (○: anodized, 0.0 MR, dry; □: anodized 0.17 MR, dry; ●: etched, 0.0 MR, dry; ■: etched, 0.17 MR, dry; ◆: etched, 0.17 MR, wet).

anodized aluminum is much more articulated than for the etched aluminum. The dimensions of the anodized pore (100 nm deep and 20 nm wide) are such that multiple polystyrene molecules could penetrate or occupy the pore. The etched pores have greater width of about 40 nm, but are only about 5 nm deep, less than d_e or R_g for polystyrene. Therefore the surface topography from the anodized treatment adds an additional significant length scale to the polymer structure developing at the surface and can strongly influence the fracture energy dissipation process in the interfacial region. Surface irregularities of the aluminum surface will direct some of the peel force into other directions and the entangled polystyrene chains in the pores can then act as stiffeners.

Additionally, XPS results in Table 1 show the oxide layer developed by the anodized aluminum incorporates phosphate, while the chromic-sulfuric acid etched aluminum does not incorporate any chromium. Consequently as pointed out by Venables [3], the oxide layer is more hydrophobic for anodized than for acid etched aluminum. The net effect is to eliminate fracture energy Regime I and part or perhaps all of Regime II for acid anodized joints. The added constraint of the

TABLE 1 Chemical Composition Analysis of Aluminum Surfaces Using XPS

Surface treatment	Relative concentration (%)				
	O_{1s}	Al_{2p}	C_{1s}	P_{2s}	Cr_{2p}
Aluminum As-received	47.0	33.6	19.4	NA	NA
Chromic sulfuric etched	46.2	39.4	14.4	NA	NA
Phosphoric acid anodized	52.4	32.0	13.5	2.1	NA

anodized pore in part limits mobility of the polystyrene chain and contributes to moving the transition points to the various regimes toward smaller grafted polystyrene thickness.

CONCLUSIONS

The molecular and micro-mechanical processes that impart strength and stability to an adhesive joint when stressed under various environmental conditions were studied with a model system of polystyrene bonded to high purity aluminum using controlled amounts of styrl silane coupling agent. On a relatively smooth, acid etched, aluminum oxide surface, it is necessary to provide a sufficient density of surface binding sites to provide a grafted or tethered layer of polymer that exceeds the average distance between entanglement points for that polymer in order to obtain maximum fracture resistance. This condition holds true whether the joint is exposed to dry or wet environmental conditions.

While there is an additional fracture mechanism, surface hydrolysis of the siloxane bond in the wet test condition, the length scales for aluminum bound polystyrene to give good adhesion to the bulk polystyrene in the joint follow behavior previously found for blocks of styrene homopolymers that are annealed together. The ratio of wet to dry fracture energy approaches zero when no silane is added, but reaches a plateau of about 0.82 at silane to polystyrene mole ratios above 0.17 where the dominant fracture mechanism is craze formation. In the intermediate region the ratio may increase linearly with grafted polystyrene thickness and equivalently the square root of the silane to polystyrene mole ratio.

On an anodized aluminum surface with well developed and deep structures where mechanical interlocking can occur and where the surface oxide is more hydrophobic, the tightly bound layer of polymer is not necessary. The length scale needed for adhesion stability and the mechanism through which the mechanical interlocking occurs needs further investigation.

REFERENCES

[1] Gutowski, W. S., *J. Adhesion* **79**, 445–482 (2003).
[2] Smith, L. V., Campbell, Benjamin D., and Peterson, K., *Int. SAMPE Tech. Conf.* **33**, 998–1008 (2001).
[3] Venables, J. D., *J. Mater. Sci.* **19**, 2431–2453 (1984).
[4] Zanni-Deffarges, M. P. and Shanahan, M. E. R., *Int. J. Adhesion Adhesives* **15**, 137–142 (1995).
[5] Jewtha, J. K. and Kinloch, A. J., *J. Adhesion* **61**, 71–95 (1997).
[6] Korenberg, C. F., Kinloch, A. J., and Watts, J. F., *J. Adhesion* **80**, 169–201 (2004).
[7] Rider, A. N. and Arnott, R., *J. Adhesion* **75**, 203–228 (2001).
[8] Zhang, S., Panat, R., and Hsia, K. J., *J. Adhesion Sci. Technol.* **17**, 1685–1711 (2003).
[9] Mittal, K. L., (Ed.) *Silanes and Other Coupling Agents*, (VSP, Utrecht, 2000), Vol. 2.
[10] Blohowiak, K. Y., Osborne, J. H., Krienke, K. A., Sekits, D. F., *Int. SAMPE Tech. Conf.* **28**, 440–446 (1996).
[11] Schnell, R., Stamm, M., and Creton, C., *Macromolecules* **31**, 2284–2292 (1998).
[12] Schnell, R., Stamm, M., and Creton, C., *Macromolecules* **32**, 3420–3425 (1999).
[13] Brown, H. R., *Macromolecules* **24**, 2752–2756 (1991).
[14] Sha, Y., Hui, C. Y., Ruina, A., and Kramer, E. J., *Macromolecules* **28**, 2450–2459 (1995).
[15] Silvestri, L., Brown, H. R., Carra, Ste., and Carra, Ser., *J. Chem. Phys.* **119**, 8140–8148 (2003).
[16] Namkanisorn, A., Ghatak, A., Chaudhury, M. K., and Berry, D. H., *J. Adhesion Sci. Technol.* **15**, 1725–1745 (2001).
[17] Product Information (Data Sheet), *Dow Corning® Z-6032 Silane*, Dow Corning Corp., Michigan (1996).
[18] Pocius, A. V, *J. Adhesion* **39**, 101–121 (1992).
[19] Critchlow, G. W. and Brewis, D. M., *Int. J. Adhesion Adhesives* **16**, 255–275 (1996).
[20] Digby, R. P. and Shaw, S. J., *Int. J. Adhesion Adhesives.* **18**, 261–264 (1998).
[21] Shimizu, K., Brown, G. M., Kobayashi, K., Skeldon, P., Thompson, G. E., and Wood, G. C., *Corrosion Sci.* **40**, 1049–1072 (1998).
[22] Schultz, J. and Nardin, M. in *Adhesion Promotion Techniques Technological Applications*, K. L. Mittal and A. Pizzt, (Eds.) (Marcel Dekker, New York, 1999).
[23] Plueddemann, E. P., *Silane Coupling Agents*, (Plenum Press, New York, 1982).
[24] Xu, Z., Hadjichristidis, N., Fetters, L. J., and Mays, J. W., *Adv. Polym. Sci.* **120**, 1–50 (1995).
[25] Onogi, S., Masud, T., and Kitagawa, K., *Macromolecules* **3**, 109–116 (1970).
[26] Wagner, C. D., Riggs, W. M., Davis, L. E., Moulder, J. F., and Muilenberg, G. E., *Handbook of X-ray Photoelectron Spectroscopy* (Perkin Elmer Corporation, Eden Prairie, Minnesota, 1979), pp. 52–53.
[27] Box, G. P., Hunter, W. G., and Hunter, J. S., *Statistics for Experimenters* (John Wiley & Sons, New York, 1978), Chap. 5, pp. 137–145.
[28] Brown, H. R., *Macromolecules* **34**, 3720–3724 (2001).